Fluorescein Angiography Findings in Eyes With Lamellar Macular Hole and Epiretinal Membrane Foveoschisis

Roberto dell'Omo,[1] Mariaelena Filippelli,[1] Serena De Turris,[2] Luca Cimino,[3] David H. Steel,[4] Carlos E. Pavesio,[5] Andrea Govetto,[6] Ismael Chehaibou,[7] Francesco Parmeggiani,[8] Mario R. Romano,[9] Lucia Ziccardi,[10] Enza Pirozzi,[11] and Ciro Costagliola[1]

[1]Department of Medicine and Health Sciences "Vincenzo Tiberio," University of Molise, Campobasso, Italy
[2]Eye Clinic, Polytechnic University of Marche, Ancona, Italy
[3]Ocular Immunology Unit, Azienda USL-IRCCS of Reggio Emilia, Reggio Emilia, Italy
[4]Department of Ophthalmology, Sunderland Eye Infirmary, Sunderland, United Kingdom and Newcastle University, Sunderland, Newcastle, United Kingdom
[5]Moorfields Eye Hospital, London, United Kingdom
[6]Fatebenefratelli-Oftalmico Hospital, ASST-Fatebenefratelli-Sacco, Milan, Italy
[7]Université de Paris, Ophthalmology Department, AP-HP, Hôpital Lariboisière, Paris, France
[8]Department of Morphology, Surgery and Experimental Medicine, University of Ferrara, Ferrara, Italy
[9]Department of Biomedical Science, Humanitas University, Pieve Emanuele, Milan, Italy
[10]Neurophysiology and Neurophthalmology Unit, IRCCS- Fondazione Bietti, Rome, Italy
[11]Institute of Ophthalmology, Santa Croce e Carle Hospital, Cuneo, Italy

Correspondence: Roberto dell'Omo, Department of Medicine and Health Sciences "Vincenzo Tiberio," University of Molise, Via Francesco De Sanctis 1, 86100, Campobasso, Italy;
roberto.dellomo@unimol.it.

Purpose. The purpose of this paper was to study fluorescein angiography (FA) findings in eyes with lamellar macular hole (LMH), and epiretinal membrane (ERM) foveoschisis.

Methods. In this prospective, observational case series, 46 eyes of patients affected by either LMH or ERM foveoschisis were examined using optical coherence tomography (OCT) and FA. All patients underwent a comprehensive ophthalmological examination and a general workup to exclude uveitis. Main outcome measures were: presence of FA abnormalities, measurements of the areas of vascular leakage, and intensity of pixels in the vitreous.

Results. Twenty-four (52.2%) eyes with LMH and 22 (47.8%) with ERM foveoschisis were studied. Overall, FA abnormalities were found in 20 (83.3%) eyes with LMH and 18 (81.8%) with ERM foveoschisis. The median areas of posterior pole and peripheral leakage were 7.52 vs. 1.07 mm^2 ($P = 0.03$) and 21.8 vs. 3.74 mm^2 ($P = 0.02$) in the LMH and ERM foveoschisis group, respectively. Disk hyperfluorescence was found in 8 and 4 eyes and perivascular leak in 10 and 4 eyes with LMH and ERM foveoschisis, respectively. OCT-derived measurements of vitreous intensity did not differ between the two groups, and the investigational workup for uveitis was negative in all patients.

Conclusions. Discrete areas of central and peripheral leakage are commonly found in eyes with LMH and ERM foveoschisis, whereas perivascular leak and hyperfluorescence of the disc are less frequently observed. These findings suggest that breakdown of the retinal blood barrier, involving the posterior pole and the periphery, is frequently associated with these two vitreoretinal disorders.

Keywords: lamellar macular hole, epiretinal membrane foveoschisis, epiretinal proliferation, optical coherence tomography, fluorescein angiography

The term lamellar macular hole (LMH) was introduced in 1975 by Gass,[1] who described an oval reddish macular lesion resulting from an unroofed foveal cyst in an eye with cystoid macular edema. On histological analysis, this lesion showed evidence of foveal tissue loss.

Since this original definition, the evolution of imaging techniques, especially the advent of spectral domain optical coherence tomography (SD-OCT), has renewed interest in the diagnosis of LMH and greatly expanded the possibilities for insight into its pathogenesis. Originally, SD-OCT-based features of LMH included an irregular foveal contour, a partial thickness defect of the macula with intact or disrupted outer retinal layers and two types of associated epiretinal materials[2–7]: (1) tractional epiretinal membrane (ERM) and (2) epiretinal proliferation (EP; also termed "thick,"[2] "dense"[3] membrane or LMH-associated epiretinal proliferation).[5] Histopathologic analysis has shown that myofibroblasts dominate in ERM, whereas EP is comprised primarily of fibroblasts and hyalocytes, and possesses weaker contractive properties relative to ERM.[8]
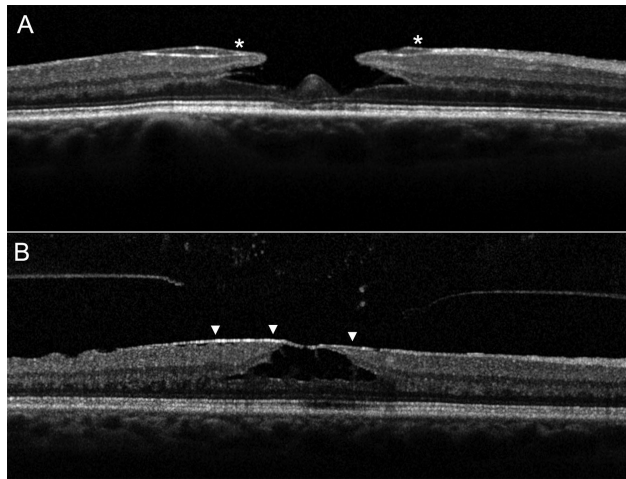
1

FIGURE 1. Spectral-domain optical coherence tomography features of lamellar macular hole (LMH) and epiretinal membrane (ERM) foveoschisis. (**A**) An LMH is characterized by irregular foveal contour, foveal cavity with undermined edges and thinning of or around the fovea. Associated pathological changes can include: epiretinal proliferation (*asterisks*), (i.e. thick, homogeneous, and isoreflective preretinal material over the internal limiting membrane [ILM]); foveal bump; and disruption of the outer retinal bands (external limiting membrane, ellipsoid zone and interdigitation zone). (**B**) An ERM foveoschisis is characterized by a contractile ERM (*arrowheads*) causing retinal wrinkling, schisis between the the outer nuclear and outer plexiform layer, and thickening at the macula.

In 2016, taking into consideration the characteristics of the epiretinal material associated with LMH and other specific features on SD-OCT imaging, Govetto et al. proposed to classify LMH in 2 types: degenerative and tractional.[9] However, Gaudric et al.[10] contended that some tractional LMHs could be not "true" LMHs but rather macular pseudoholes (MPHs) with lamellar cleavage of their edges. In fact, using en face OCT, several epicenters of contraction were visible in eyes with tractional LMH/MPH, but not in eyes with degenerative, in other words, true LMH.

More recently, a panel of vitreo-retinal experts[11] proposed a new SD-OCT-based definition of LMH. According to the panel, mandatory criteria for the diagnosis of LMH are: irregular foveal contour, foveal cavity with undermined edges, and other signs evoking a loss of foveal tissue. Conversely, the cases previously referred in the literature to as "tractional" LMH have been renamed by the panel as ERM foveoschisis (Fig. 1).

The fundamental concept at the base of this new classification[11] is that tissue loss is present exsclusively in LMH in contradistinction to ERM foveoschisis. However, OCT imaging is not fully reliable in distinguishing loss of tissue and, more importantly, is not able to provide information about its cause. Thus, it is interesting to explore the contribution that other imaging modalities can offer to study LMH and ERM foveoschisis.

Blue fundus autofluorescence (B-FAF) detected no significant differences between eyes with LMH and ERM foveoschisis (previously referred to in the literature as tractional LMH).[6,12] Both are characterized by an area of increased autofluorescence of similar size, with similar stability/progression over time. The intensity of this area does not correlate with the thickness of the residual outer retinal tissue.[12]

For the past 50 years, fluorescein angiography (FA) has proved to be an extremely valuable technique for expanding our knowledge of the pathophysiology of various retinal conditions, and has aided the diagnosis and monitoring of several macular diseases. In comparison to OCT and B-FAF, FA is invasive and has a substantially limited depth resolution; however, it is a fundamental diagnostic tool for the identification of blood retinal barrier breakdown and optic disc edema. There has been very limited data presented in the literature on FA findings in patients affected by LMH.[13,14] The purpose of this paper was to study FA findings in eyes with LMH and ERM foveoschisis in order to gain further insights into their pathogenesis.

METHODS

We conducted a prospective analysis of patients affected by LMH and ERM foveoschisis based on SD-OCT that were seen at the University of Molise, Campobasso, from March 1, 2020, to September 30, 2020. All subjects were treated in accordance with the Declaration of Helsinki. This study was approved by the Institutional Review Board of the University of Molise. Informed consent was obtained from the subjects after explanation of the nature and possible consequences of the study.

The SD-OCT criteria used to diagnose LMHs and ERM foveoschisis were those recently proposed by Hubschman and associates.[11] Specifically, an LMH had to have: (1) an irregular foveal contour; (2) a foveal cavity with undermined edges; (3) the presence of at least one other sign suggesting loss of foveal tissue, which is a pseudo-operculum, thinning of the foveal at its center, or around. Associated SD-OCT changes could include: (1) epiretinal proliferation, (2) foveal bump, and (3) ellipsoid zone disruption. Conversely, ERM foveoschisis had to show (1) contractile ERM; (2) foveoschisis at the level of Henle fiber layer (HFL) and, optionally, the presence of microcystoid spaces in the inner nuclear layer, retinal thickening, and retinal wrinkling. On OCT imaging, standard or typical ERM was defined as a highly reflective line, whereas EP was defined as a material of homogenous medium reflectivity located on the epiretinal surface[15] (see Fig. 1).

The exclusion criteria were a history of retinal detachment, ocular surgery, including uneventful cataract extraction in the last 12 months, previous pars plana vitrectomy, previous systemic and ocular inflammation, advanced age-related macular degeneration, diabetic retinopathy, central retinal vein occlusion, hypertensive retinopathy, macular telangiectasia, trauma, optic nerve diseases such as glaucoma or optic neuropaties, and a refractive error of more than –8 diopters of spherical equivalent. Particular attention was paid to exclude signs of uveits, a possible cause of secondary LMH or ERM foveoschisis.[16] Thus, an accurate search for keratic precipitates, posterior synechiae, cataract or capsular opacification (in pseudophakic eyes), and evaluation of intraocular inflammation in anterior and posterior ocular segments (according to Standardization of Uveitis Nomenclature [SUN] Working Group scoring system)[17] by experienced observers (R.d.O. and M.F.) was carried out. The presence and severity of vitreous haze, if present, was classified by the same graders according to the National Eye Institute (NEI) system.[18]

In addition, in order to exclude systemic inflammatory diseases causing ocular inflammation, an investigational workup including chest X-ray, QuantiFERON-TB Gold (QFT)
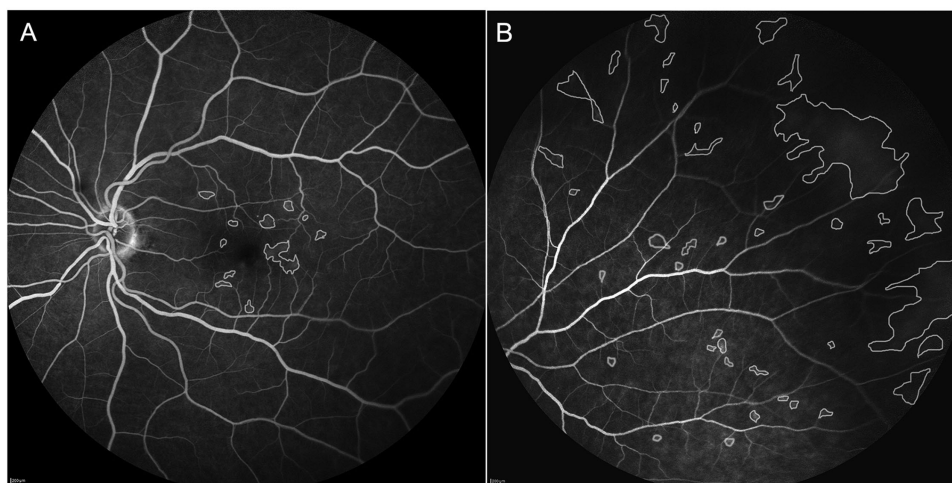
FIGURE 2. Manual outlining of the areas of leakage on fluorescein angiography images at the posterior pole (**A**) and at the periphery (**B**).

test, serological testing for syphilis, toxoplasmosis and Lyme disease, and immunological tests, including HLA-B51, antinuclear antibodies, ACE, lysozyme, interleukin-2 receptor, and antineutrophil cytoplasmic antibodies were also performed.

Subjects with any ocular condition that would interfere with good-quality image acquisition were also excluded.

All patients underwent a comprehensive ophthalmic examination. Best-corrected visual acuity (BCVA) was measured using Early Treatment Diabetic Retinopathy Study (ETDRS) charts. In addition, patient characteristics, including age, sex, lens status, and refractive error, were recorded.

Imaging

All images were collected using the Heidelberg Spectralis system HRA + OCT (Heidelberg Engineering, Heidelberg, Germany) using the 35 degree and 50 degree lenses. B-FAF (excitation wavelength at 488 nm and barrier filter at 500 nm), FA, and OCT images were obtained after pupil dilation. The SD-OCT recording protocol consisted of a sequence of 37 horizontal sections, spaced 120 µm apart, covering an area of 20 degrees or 30 degrees horizontally by 15 degrees vertically, and a sequence of 24 radial sections recorded in the high-resolution (HR) mode simultaneously with infrared (IR) images. In addition, simultaneous FA/OCT images were acquired. Multiple SD-OCT morphologic characteristics were analyzed, including the relation of the vitreous cortex with the surface of the macula (attached/detached) and with the disc (i.e. vitreopapillary adhesion [VPA], defined as a visible vitreous membrane attached to the optic disc) and the presence of disruption of the outer retinal bands (ORBs; i.e. external limiting membrane, ellipsoid, and interdigitation zones). Central foveal thickness (CFT) was defined as the thinnest vertical height from the internal limiting membrane (ILM) to the inner retinal pigment epithelium (RPE) boundary and was manually measured using the caliper function of the Heidelberg device. Macular thickness (corresponding to the mean thickness within the 5 ETDRS fields) was measured using the in-built Spectralis Software, and boundary lines were manually adjusted when necessary.

The angiography procedure involved intravenous injection of 5 mL sodium fluorescein (10%). Images of the posterior pole were taken at 1, 2, 5, 10, and 20 minutes after injection of the dye using the 35 degree lens, whereas peripheral sweeps of all quadrants were acquired using the 50 degree lens starting 5 minutes after dye injection. Two masked, trained graders (M.F. and S.D.T.) independently analyzed the images. Areas of vascular leakage, when present, were outlined and measured using the software ImageJ (freely available at http://rsb.info.nih.gov/ij/index.html)[19]; the hyperfluorescent areas corresponding to the hole and the related cysts (if present) were excluded from analysis (Fig. 2). The outline of the retinal pathology was verified by a third trained grader (R.d.O.). Pixel values were then converted into µm values using Image J, and the data were averaged between the two graders to obtain the final values used for analysis.

Quantitative Analysis of the Vitreous Using OCT

After exporting from Heidelberg Spectralis, the IR-OCT images in TIFF, using the "Export as image" function (SPECTRALIS software version 6.16.2), the images were imported into Image J. Once imported into Image J, the tool "rectangle" was used to select the OCT scan image only. Then, the OCT images were segmented manually using the "paint-brush" tool and according to the boundary definitions proposed and described by Keane and coworkers.[20] The boundaries were outlined over the entire length of each OCT image. These boundaries consisted of (1) "vitreous top," the uppermost extent of the vitreous space as visualized on OCT; (2) internal limiting membrane (ILM), the inner boundary of the neurosensory retina; (3) RPE-inner, the inner boundary of the RPE; and (4) RPE-outer, the outer boundary of the RPE (Fig. 3). The vitreous space was defined as the space between the "vitreous top" and the ILM—except in cases of partial detachment of the posterior hyaloid face, or ERM, wherein the innermost boundary was chosen. The RPE was defined as the space lying between the inner and outer boundaries of the RPE.

For each patient, 5 B radial scans (about 6 mm long) spaced 15 degrees apart and passing through the foveal center were considered for analysis. The 5 scans analysed were those with the highest signal/noise ratio among the 24-radial sections recorded for each patient. Subsequently, selecting "analyze" from the dropdown menu, the function
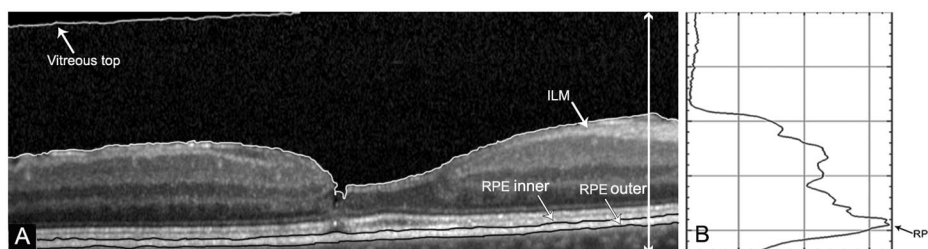
FIGURE 3. Quantitative assessment of vitreous intensity using spectral-domain optical coherence tomography (SD-OCT). (**A**) OCT B-scan after manual segmentation of the vitreous compartment and the retinal pigment epithelium (RPE; boundaries: RPE-inner to RPE-outer). (**B**) Quantification of the reflectivity levels along the *white line* shown in **A**.

"plot profile" was used to obtain a graph in which the y-axis represented "gray value" and the x-axis represented the "distance" measured in pixels. Then the function "plot options" was set on "vertical profile" in order to obtain intensity values from the choriocapillaris to the vitreous. The mean value of the intensity obtained in the vitreous space (termed "VIT-absolute intensity") and the peak value obtained in correspondence of the RPE band (termed "RPE-absolute intensity) were recorded for each scan. Then, the mean value obtained from five scans was calculated. Finally, intensity values for the vitreous and RPE spaces were expressed as a ratio (termed "VIT/RPE-relative intensity"). All segmentations and calculations were performed by two OCT graders (M.F. and S.d.T.), who were blinded to all clinical information at the time of grading.

Statistical Analysis

Clinical and imaging data were summarized with descriptive statistics. The median scores were calculated and compared for each parameter of the visual function and imaging measurements. The Wilcoxon, Mann–Whitney U, and Fisher exact tests were used to compare clinical and OCT parameters between the two groups. FA findings potentially influencing the presence of LMH were studied using stepwise logistic regression analysis. The interrater agreement between graders was determined with intraclass correlation coefficients (ICCs). Statistical analysis was performed using MedCalc version 11.5.1 (MedCalc Software, Mariakerke, Belgium), with statistical significance set at $P < 0.05$.

RESULTS

A total of 46 eyes from 46 patients that met both the inclusion criteria and our definition of LMH and ERM foveoschisis were enrolled. The mean age ($\pm$ SD) was 69.8 ± 8.5 years. Of these 46 patients, 16 (34.8%) were men and 30 (65.2%) were women. Mean refractive error (spherical equivalent) was -1.75 ± 1.50 and -2.25 ± 2.00 for the study and fellow eyes, respectively; 28 of the study eyes were phakic and 18 pseudophakic; among the fellow eyes 32 were phakic and 14 pseudophakic. OCT images showed LMH in 24 eyes (52.2%) and ERM foveoschisis in 22 eyes (47.8%). Sixteen (66.7%) of the eyes with LMH presented with both EP and ERM. A macular ERM was found in 14 cases (58.3%) among fellow eyes of the LMH group, and in 4 cases (18.2%) among fellow eyes of the ERM foveoschisis group; whereas EP was found in none of the fellow eyes in either group.

The group with LMH ($N = 24$) and the group with ERM foveoschisis ($N = 22$) differed in the following variables: logMAR BCVA (0.32 ± 0.24 vs. 0.15 ± 0.12, $P < 0.001$), CFT (166.9 ± 38.4 vs. 208.4 ± 24.8, $P = 0.0002$), and disruption of the ORB, which was noted in 14 eyes with LMH and in 2 eyes with ERM foveoschisis ($P < 0.0006$). Macular thickness was 343 ± 69.3 in the LMH group and 390.8 ± 39 in the ERM foveoschisis group ($P = 0.03$). A posterior cortex detached from the macular area was visible on OCT images in 6 cases (25%) with LMH and in 10 cases (45.4%) with ERM foveoschisis ($P = 0.42$). A VPA was found in five eyes with LMH (20.8%) and in nine (40.9%) eyes with ERM foveoschisis ($P = 0.2$; Table).

Investigational workup for uveitis was negative in all patients. However, four patients in the LMH group reported a family history positive for autoimmune disease. Slit-lamp examinaton revealed no signs of anterior inflammation in any eye. Neither vitritis nor choroidal/retinal scarring were found in any patient.

Fluorescein Angiography Findings

Areas of central (i.e. within the first order vascular arcades) leakage were observed in 20 eyes (83.3%) with LMH and in 18 eyes (81.8%) with ERM foveoschisis ($P = 1.0$), whereas areas of peripheral leakage were found in 20 eyes (83.3%) with LMH and 12 eyes (54.5%) with ERM foveoschisis ($P = 0.05$). The areas of leakage usually consisted of foci with linear diameter < 150 μm at the posterior pole and larger areas (linear diameter >150 μm) at the periphery (Figs. 4–9).

Ten (41.7%) and four (18.2%) eyes in the LMH and ERM foveoschisis group, respectively, showed focal perivascular leak ($P = 0.11$). This perivascular leak affected exclusively the retinal veins (Fig. 6). Hyperfluorescence of the disc was observed in eight cases (33.3%) in the LMH and in four cases (18.2%) in the ERM foveoschisis group ($P = 0.32$). Overall FA abnormalities were found in 38 of the 46 studied eyes (82.6%); 20 (83.3%) with LMH and 18 (81.8%) with ERM foveoschisis (Fig. 10).

Among the fellow eyes of the LMH group, 18 (75%) showed central leakage, 20 (83.3%) showed peripheral leakage, 6 (25%) showed perivascular leak, 6 (25%) showed hyperfluorescence of the disc, and 4 (16.7%) showed no FA abnormalities; in all cases, the eyes that presented with hyperfluorescence of the disc or perivascular leak also showed central or peripheral leakage. Among the fellow eyes of the ERM foveoschisis group, 8 (36.4%) showed central leakage, 6 (27.3%) showed peripheral leakage, 2 (9%) showed perivascular leak, 2 (9%) showed hyperfluorescence of the disc, and 10 (45.4%) showed no FA abnormalities. As

TABLE. Spectral-Domain Optical Cohrence Tomography and Fluorescein Angiography Findings of the Sample

	LMH $n = 24$	ERM Foveoschisis $n = 22$	LMH Fellow $n = 24$	ERM Foveoschisis Fellow $n = 22$	LMH vs. ERM Foveoschisis	LMH vs. Fellow	ERM Foveoschisis vs. Fellow P Value[*]	LMH Fellow vs. ERM Foveoschisis Fellow
Presence of EP	24 (100%)	0	0	0	0.000000001	0.000000001	1.00	1.00
Presence of ERM	16 (66.7%)	22 (100%)	14 (58.3%)	4 (18.2%)	1.00	0.017	0.00000001	0.0072
Posterior cortex detached from macula	6 (25%)	10 (45.4%)	8 (33.3%)	10 (45.4%)	0.42	0.75	1.00	0.54
Vitreopapillary adhesion	5 (20.8%)	9 (40.9%)	7 (29.2%)	8 (36.4%)	0.2	0.74	1.00	0.75
Intraretinal hyperreflective dots	24 (100%)	12 (54.5%)	24 (100%)	2 (9%)	0.00015	1.00	0.0027	<0.000000001
Disruption of outer retinal bands	14 (58.3%)	2 (9%)	0	0	0.0006	0.000008	0.48	1.00
No FA abnormalities	4 (16.7%)	4 (18.2%)	4 (16.7%)	10 (45.4%)	1.00	1.00	0.10	0.054
Central leakage	20 (83.3%)	18 (81.8%)	18 (75%)	8 (36.4%)	1.00	1.00	0.005	0.016
Peripheral leakage	20 (83.3%)	12 (54.5%)	20 (83.3%)	6 (27.3%)	0.054	1.00	0.12	0.00025
Hyperfluorescence of the disc	8 (33.3%)	4 (18.2%)	6 (25%)	2 (9%)	0.32	0.75	0.66	0.24
Perivascular leak	10 (41.7%)	4 (18.2%)	6 (25%)	2 (9%)	0.11	0.35	0.66	0.24

EP = epiretinal proliferation; ERM = epiretinal membrane; FA = fluorescein angiography; LMH = lamellar macular hole; n = number of eyes.
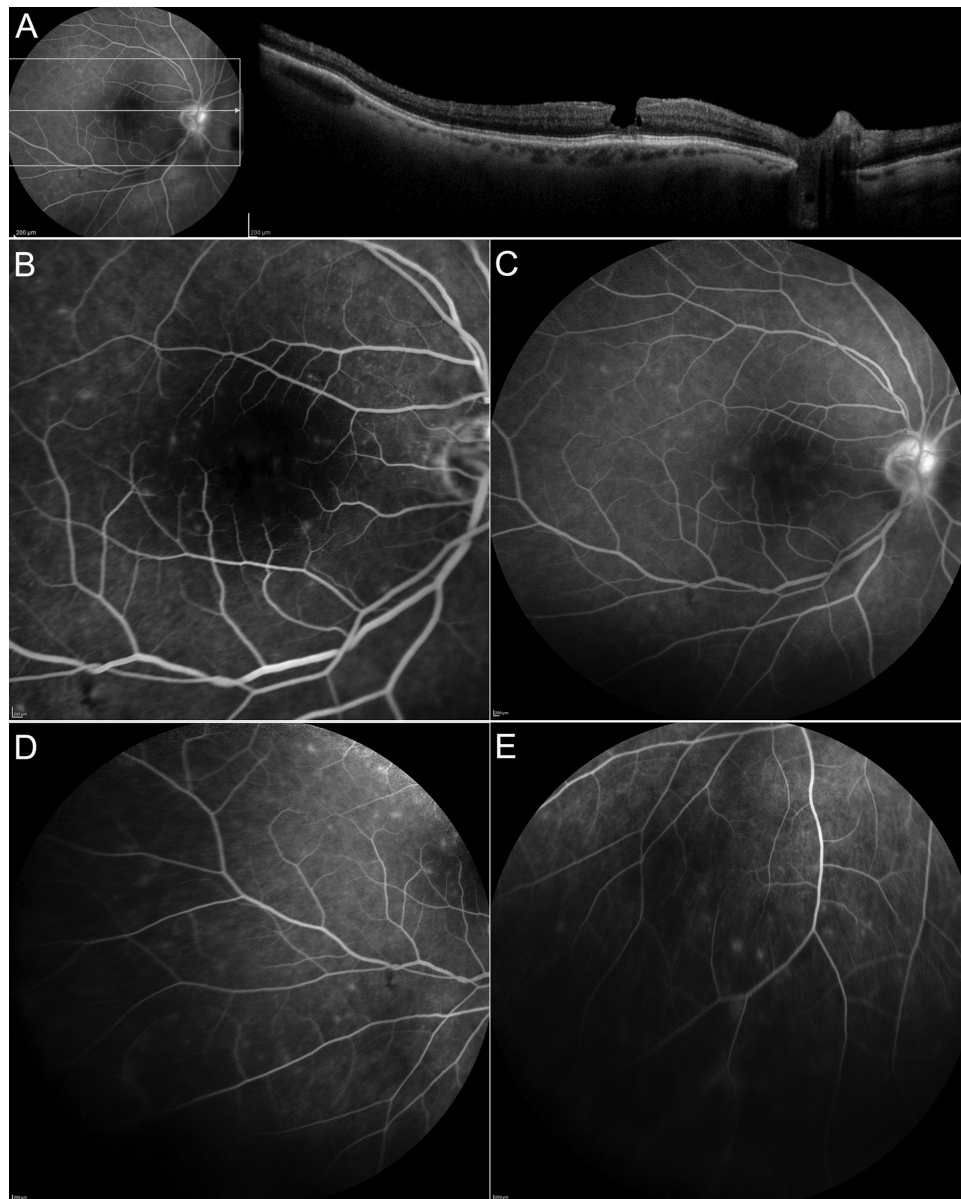[*]Fisher exact test.

FIGURE 4. Fluorescein angiography (FA) and spectral-domain optical coherence tomography (SD-OCT) findings in a patient with lamellar macular hole (LMH). (**A**) The OCT image (with the related FA picture showing the level of the OCT scan) shows an LMH characterized by irregular foveal contour, foveal cavity with undermined edges, thinning of the fovea, epiretinal proliferation, and focal disruption of the outer retinal bands. No sites of vitreoretinal traction are observed either in the retinal area scanned or at the level of the optic disc. Fluorescein angiography shows discrete areas of leakage at the posterior pole (**B**) and at the periphery (**C, D, E**) along with hyperfluorescence of the disc and focal vasculitis of the veins.

with the LMH fellow group, all the eyes showing hyperfluorescence of the disc and perivascular leak also presented with central or peripheral leakage. Overall, FA abnormalities were found in 32 (69.6%) fellow eyes, 20 (83.3%) in the LMH group and 12 (54.5%) in the ERM foveoschisis group.

Areas of peripheral retinal nonperfusion or vascular alterations, such as capillary dropout, telangiectasia, collateral vessels and microaneurysms, and retinal/disc neovascularization, were not observed in any patient. The median areas of posterior pole leakage were 7.52 mm^2 (95% confidence interval [CI] = 1.82–9.20) and 1.07 mm^2 (95% CI = 0.83–2.1, P = 0.03); whereas the median areas of peripheral leak-

age were 21.8 mm^2 (95% CI = 3.0–38.0) and 3.74 mm^2 (95% CI = 1.03–15.51, P = 0.02) in the LMH and ERM foveoschisis group, respectively. OCT scans at the posterior pole showed the presence of hyperreflective dots (HRDs) scattered troughout the inner retinal layers (Figs. 7, 8). In the LMH group, HRD were noted in all study and fellow eyes; in the ERM foveoschisis group HRD were found in 12 (54.5%) study eyes and in only 2 (9%) fellow eyes. Stepwise logistic regression analysis (independent variables in the model: posterior pole leakage, peripheral leakage, perivascular leak, and hyperfluorescence of the disc) showed that the only FA finding associated with the LMH was peripheral leakage (P = 0.03).
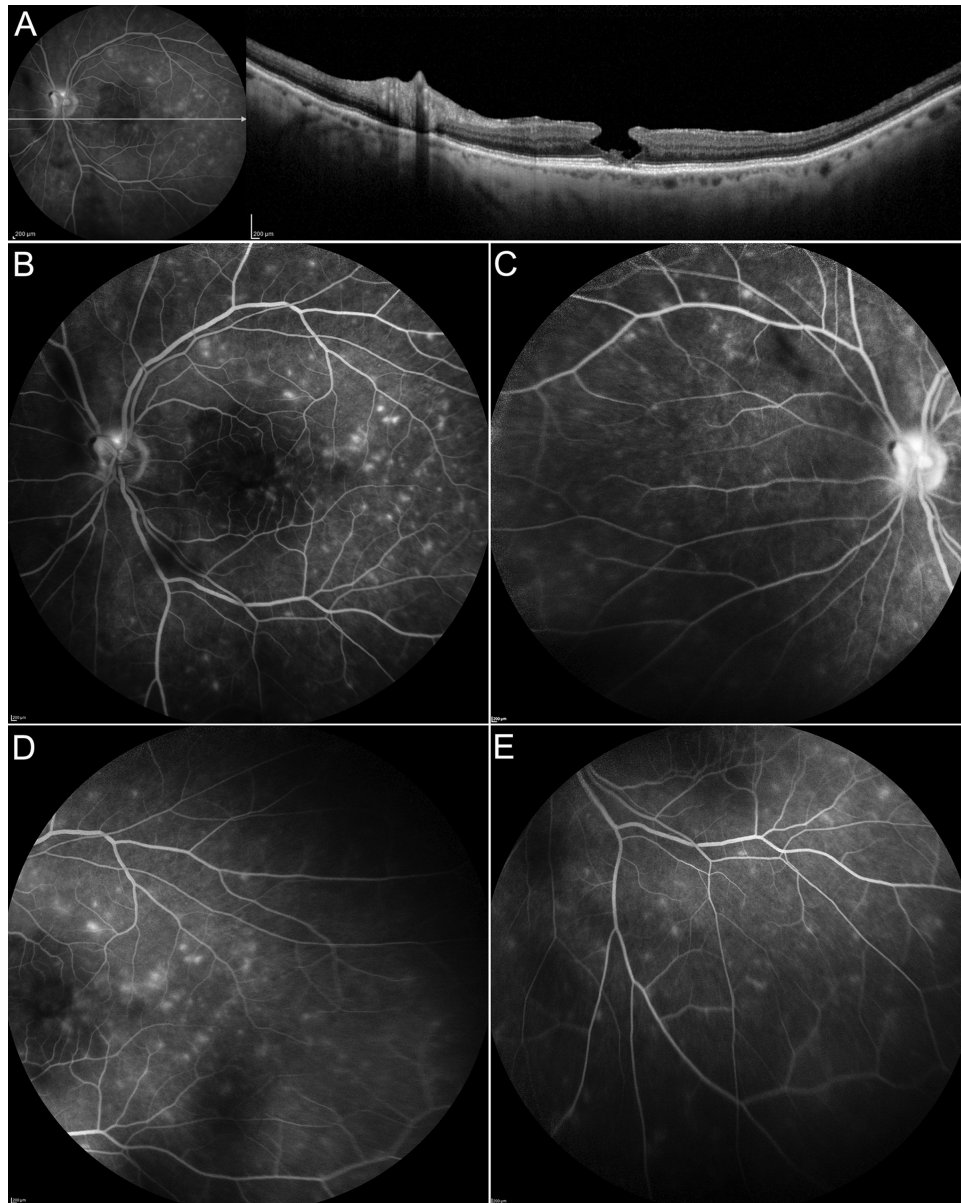
Figure 5. Fluorescein angiography (FA) and spectral-domain optical coherence tomography (SD-OCT) findings in a patient with lamellar macular hole (LMH). (**A**) The OCT image (with the related FA picture showing the level of the OCT scan) shows an LMH characterized by irregular foveal contour, foveal cavity with undermined edges, thinning of the fovea, epiretinal proliferation, foveal bump, and focal disruption of the outer retinal bands. No sites of vitreoretinal traction are observed in the retinal area scanned. Fluorescein angiography shows multiple foci of leakage scattered throughout the posterior pole (**B**) and the periphery (**C, D, E**) along with hyperfluorescence of the disc **C**.

OCT-Derived Measurements of Vitreous Intensity

No significative differences of VIT/RPE-relative intensity values were found between the study eyes in the LMH versus ERM foveoschisis group (0.06 ± 0.03 vs. 0.08 ± 0.05, $P = 0.2$), and between LMH and fellow and ERM foveoschisis and fellow eyes, respectively (0.05 ± 0.03 vs. 0.08 ± 0.03, $P = 0.7$).

Interrater Agreement

The ICC between observers for the grading of leakage areas was 0.95 (95% CI = 0.92–0.99) for the posterior pole and 0.86 (95% CI = 0.83–0.99) for the periphery.

Discussion

The pathogenetic mechanisms leading to the formation of LMH and ERM foveoschisis are not completely understood. Several theories have been proposed, including the union of intraretinal cysts,[1] aborted formation of full-thickness macular hole,[12,21,22] centrifugal traction of ERMs,[23] vitreo-foveal traction,[24] and proliferation of vitreous remnants and Müller cells on the epiretinal surface.[3,10,15]

It is thought that, differently from ERM foveoschisis, LMH is associated with foveal tissue loss,[11] but in vivo analyses, for instance OCT imaging, are not reliable in distinguishing loss of tissue, which can only be truly confirmed with histological studies.
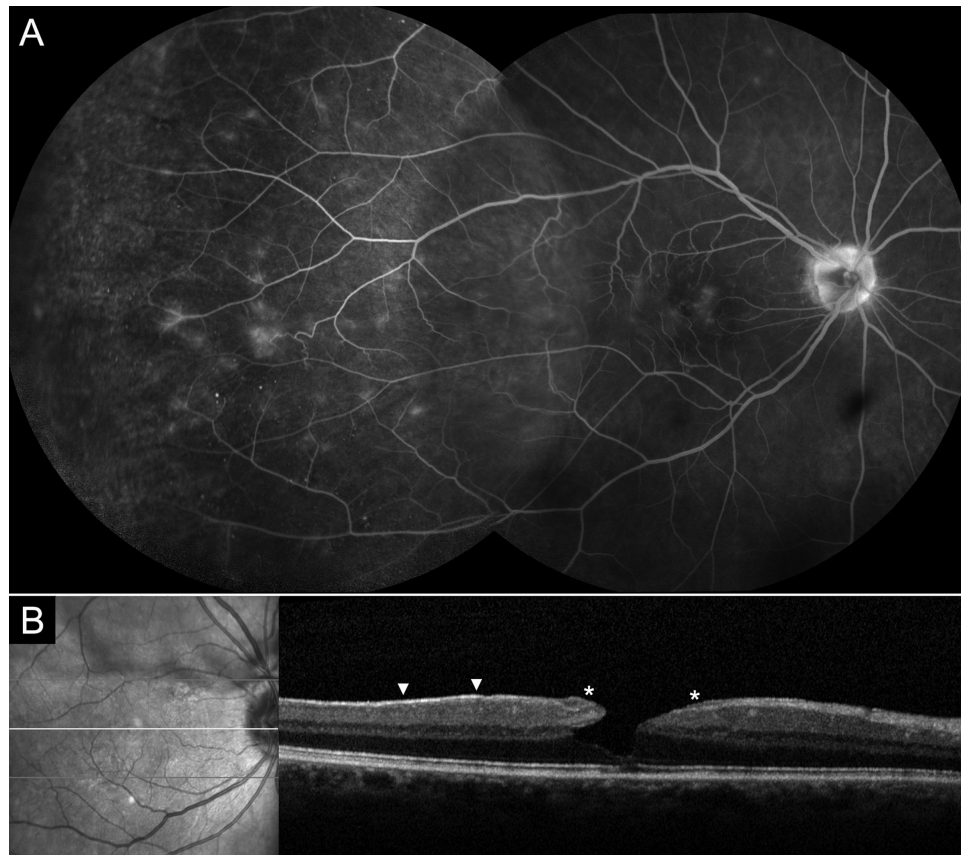
FIGURE 6. Fluorescein angiography (FA) and spectral-domain optical coherence tomography (SD-OCT) findings in a patient with lamellar macular hole (LMH). (**A**) Discrete areas of focal leakage are visible at the posterior pole and at the periphery along with hyperfluorescence of the disc and focal vasculitis of the veins (**B**) the OCT scan shows a LMH with irregular foveal contour, foveal cavity with undermined edges, thinning of the fovea with associated disruption of the outer retinal bands, epiretinal proliferation (*asterisks*), and a thin epiretinal membrane not causing traction (*arrowheads*). No sites of vitreoretinal traction are observed in the macular area scanned by OCT.

Similarly, the pathogenetic mechanism leading to the formation of EP and ERM (generally associated with LMH and ERM foveoschisis, respectively) is not completely elucidated. Immunocytochemical and ultrastructural analyses have revealed that the constituents of these epiretinal materials are similar, although with a predominance of fibroblasts and hyalocytes in EP and of myofibroblasts in ERM.[3,8] On the basis of SD-OCT, both LMH and ERM foveoschisis feature an alteration of the foveal contour that is, however, characterized by a cavity with undermined edges in LMH, and by a sharp-edged split of the neurosensory retina in ERM foveoschisis.[5,9,11] Nevertheless, mixed cases are not uncommon, and concomitant ERM and EP are frequently found in LMH.[6–8,10,25] On B-FAF, another noninvasive imaging modality, both LMH and ERM foveoschisis show an area of increased autofluorescence, the diameters and changes over time of which do not differ between the two disorders.[6]

To gain further insight into the pathogenesis of these vitreomacular pathologies, we carried out multimodal analysis, including FA. Despite being an invasive procedure, FA has the unique advantage of being able to detect breakdown of the blood retinal barriers, even if collections of intra- and subretinal fluid, which may be detectable by OCT, have not yet occurred. Furthermore, FA may show perivascular leakage and disc hyperfluorescence even in the absence of overt, abnormal ophthalmoscopic signs of disc abnormalities, including hyperemia or swelling.

Our study found that breakdown of the blood inner retinal barrier involving the posterior pole is a common occurrence in eyes with both LMH and ERM foveoschisis. Conversely, areas of abnormal leakage in the periphery, hyperfluorescence of the disc, and perivenous leak are more commonly seen in eyes with LMH. The presence of vascular leakage at the posterior pole in eyes with ERM foveoschisis was expected. Previous studies have shown that ERM may alter the morphology, location, and permeability of the retinal vasculature due to antero-posterior and tangential traction, with resulting leakage of fluorescein dye.[26,27] The concomitant presence of ERM and EP in more than half of the eyes with LMH may also explain the leakage at the posterior pole observed in these cases. However, macular leakage was also found in the eyes affected by LMH without concomitant ERM (i.e. cases without tractional changes exerted by an epiretinal membrane). No signs of vascular distortion or tortuosity were found in these cases. It is possible that the leakage at the posterior pole observed in these cases was secondary to vitreous traction. Indeed, we found posterior vitreous cortex apparently attached to the macula on OCT in 75% and 54.6%, and leakage in the macular area in 83.3% and 81.8% of the eyes in the LMH and ERM foveoschisis group. However, no signs of classic vitreomacular traction syndrome or tractional cystoid macular edema[28] were found on OCT imaging in any of the eyes examined. Furthermore, central leakage is typically
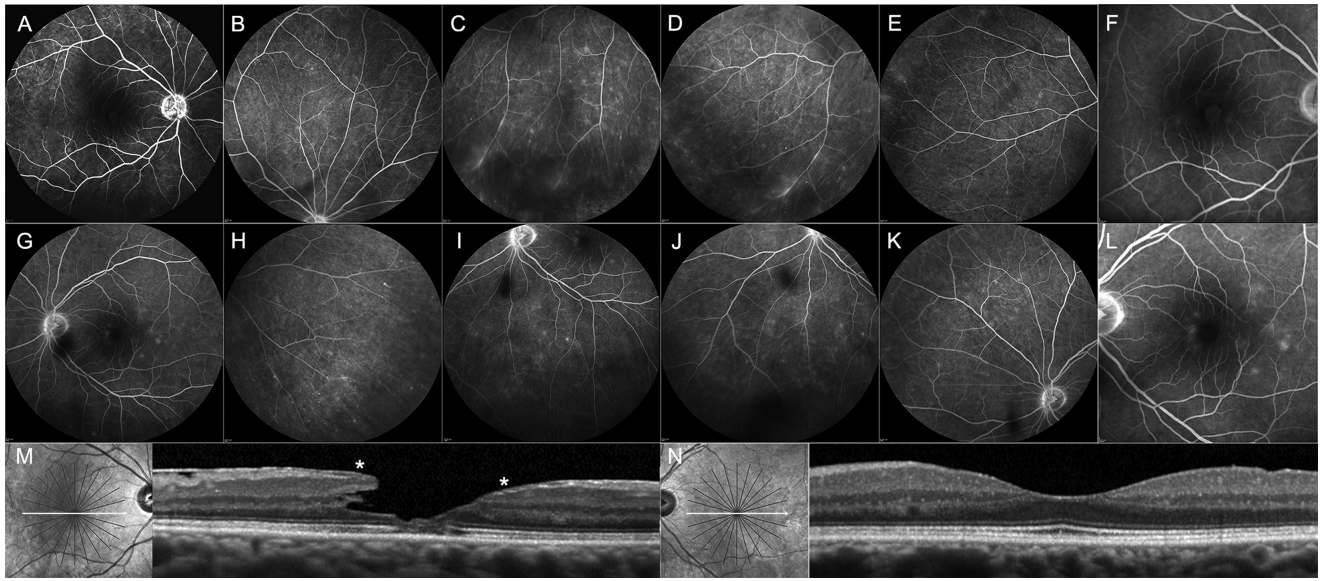
FIGURE 7. Fluorescein angiography (FA) and spectral-domain optical coherence tomography (SD-OCT) findings in a patient with lamellar macular hole (LMH) in OD and a thin epiretinal membrane (ERM) in OS. (**A–F**) In the eye with LMH, areas of leakage at the posterior pole and periphery, along with focal vasculitis and hyperfluorescence of the disc, are visible. (**G–L**) Areas of leakage at the posterior pole and periphery, although less prominent, are noted in the fellow eye as well. (**M**) The OCT image of the LMH (with the related infrared pic showing the level of the OCT scan) shows irregular foveal contour, foveal cavity with undermined edge on the temporal aspect of the fovea, foveal thinning, epiretinal proliferation (*asterisks*) along with tractional epiretinal membrane on the temporal aspect of the macula and disruption of the outer retinal bands. (**N**) The OCT image of the fellow eye shows a mildly undulated inner retinal profile on the temporal aspect of the macula due to a thin ERM. Numerous hyperreflective dots are visible.
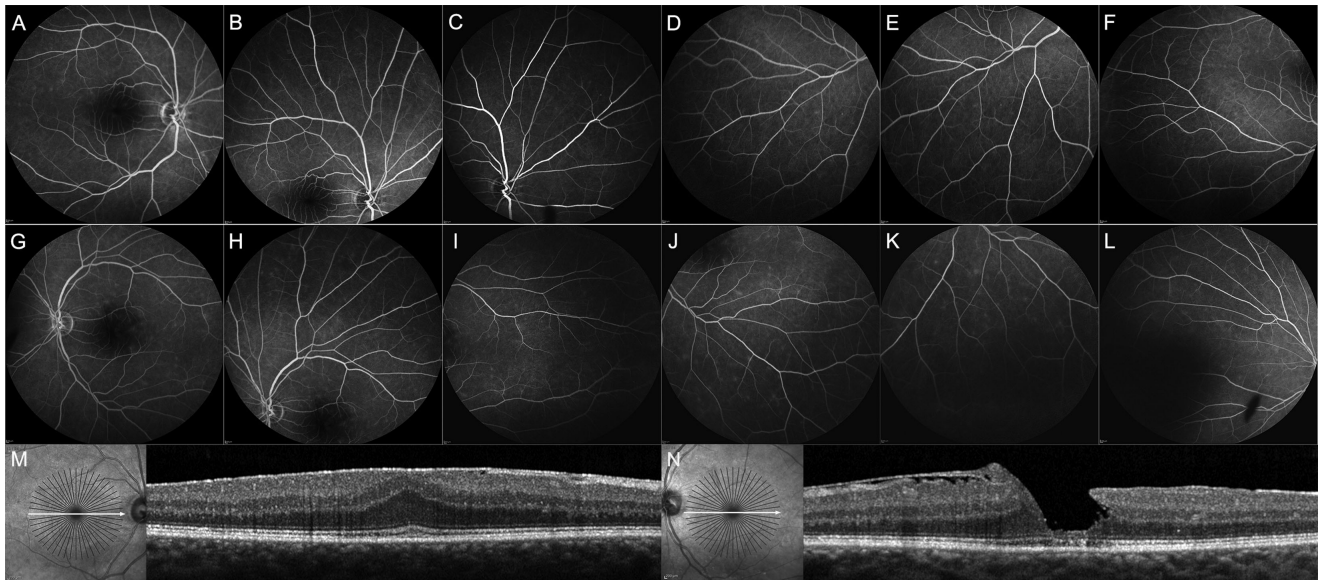

FIGURE 8. Fluorescein angiography (FA) and spectral-domain optical coherence tomography (SD-OCT) findings in a patient with an epiretinal membrane (ERM) in OD and lamellar macular hole (LMH) in OS. (**A–F**) In OD, areas of leakage at the posterior pole and a few, faint, and discrete areas of leakage at the periphery are visible. (**G-L**) In the OS, affected by LMH, the discrete areas of leakage at the posterior pole and periphery are more prominent. (**M**) The OCT image of OD (with the related infrared picture showing the level of the OCT scan), shows an ERM causing traction and thickening of the macula. Because of the antero-posterior traction and distortion exerted by the ERM, the inner retinal layers are visible at the fovea. (**N**) The OCT image of the LMH shows an irregular foveal contour, foveal cavity with an undermined edge and thinning at the fovea, disruption of the outer retinal bands, and epiretinal proliferation on both foveal sides, that is in continuity with an ERM on the nasal aspect of the macula. Numerous hyperreflective dots are visible in both OCT scans whereas no sites of vitreoretinal traction are observed in the macular area in either eye.
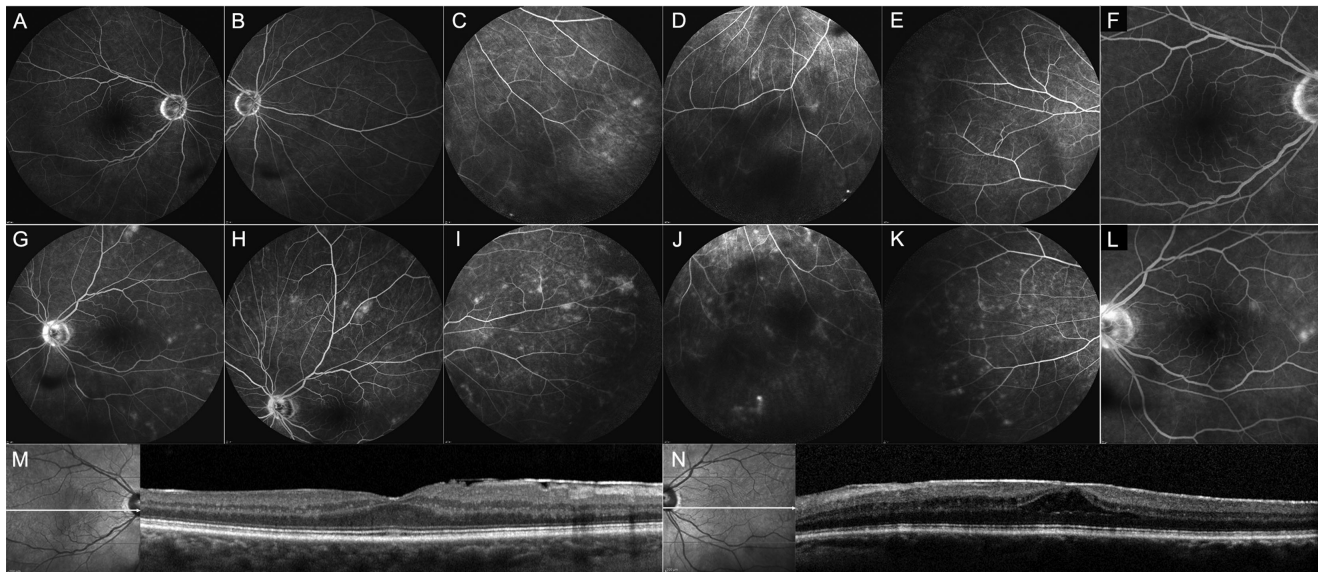
FIGURE 9. Fluorescein angiography (FA) and spectral-domain optical coherence tomography (SD-OCT) findings in a patient with epiretinal membrane (ERM) in OD and ERM foveoschisis in OS. (**A–F**) Faint areas of leakage at the posterior pole, along with hyperfluorescence of the disc and discrete peripheral areas of leakage, are visible on FA images in OD. (**G–L**) The areas of leakage and the hyperfluorescence of the disc are more prominent in OS, where focal vasculitis is also visible. (**M**) The OCT image of the OD (with the related infrared picture showing the level of the OCT scan) shows an ERM causing retinal wrinkling on the nasal aspect of the macula. (**N**) The OCT image of OS shows ERM foveoschisis characterized by schisis between the the outer nuclear and the outer plexiform layer, thickening of the macula, and microcystoid spaces in the inner nuclear layer. No sites of vitreoretinal traction are observed in the macular area in either eye.

absent on FA imaging in case of tractional cystoid macular edema.[28]

In addition to leakage at the posterior pole, we found leakage in the peripheral retina in several cases of this series and mostly in the eyes with LMH. The peripheral leakage was not associated with areas of hypoperfusion or vascular alterations, such as capillary dropout, telangiectasia, collateral vessels, microaneurysms, or neovascularization in any of the cases.

Some of the eyes with central and peripheral leakage, also showed hyperfluorescence of the disc and perivenous leak. Generally, hyperfluorescence of the disc may be seen in the setting of diabetic retinopathy, retinal vein occlusion, hypertensive retinopathy, and optic neuropaties (i.e. pathologies that were within the exclusion criteria of this study). Other pathologies that may show hyperfluorescence of the disc (i.e. papillophlebitis and retinal vein prethrombosis) are usually unilateral, occur more frequently in young patients, and are characterized by edema of the optic disc and perivenous hemorrhages. None of the eyes in this study presented with ophthalmoscopically or fundus imaging detectable disc edema or retinal hemorrhages. Irvine-Gass syndrome following cataract surgery may be another potential cause of disc hyperfluorescence and breakdown of blood retinal barriers resulting in vascular leakage on FA.[29] This syndrome is characterized by pseudophakic cystoid macular edema generally occuring weeks to months after surgery.[29,30] In this series, FA abnormalities were found in 70 of 92 eyes examined (76%) and only 32 (34.8%) of these eyes were pseudophakic. Furthermore, eyes with history of ocular surgery (including uneventful cataract extraction) in the 12 months preceding the enrollment into the study were excluded. Thus, the hypothesis that Irvine-Gass syndrome could account for the blood retinal barrier breakdown observed in the eyes of this series, is unlikely.

Perivascular leak caused by retinal vasculitis usually occurs as a manifestation of an underlying systemic condition or ocular syndrome[31]; alternatively, retinal vessels can also be involved as primary isolated or single-organ vasculitis, a category recently included in the 2012 Revised International Chapel Hill Consensus Conference Nomenclature of Vasculitides.[32] Unlike the condition idiopathic retinal vasculitis, in which the presence of phlebitis was reported in 100%,[33] vitreous cells in 58–100%,[33,34] and ischemic lesions in 21–37% of cases,[31,34,35] our study found no evidence of vitreous cells nor signs of hypoperfusion/ischemia in any of the patients examined. Furthermore, perivenous leak was detected in only 30.4% of the study eyes of our series. We have found only two reports in the literature,[36,37] examining two patients, which describe an association between vasculitis-like abnormalities observed on FA and sites of vitreoretinal traction observed on OCT. One of these two patients had a history of uveitis related to polymyalgia rheumatica.[36] Preoperatively, FA in this patient revealed cystoid macular edema and dye leakage in the peripapillary and superior midperipheral fundus corresponding to the areas of vitreo-retinal traction on OCT. However, FA was not repeated after surgery, thus it is uncertain whether the pathological leakage observed before surgery was due to vitreoretinal traction or to the underlying uveitis. Neither hyperfluorescence of the disc nor leakage or vasculitis in the peripheral retina were reported in any of the abovementioned studies.[36,37] Notably and differently from the studies cited before, signs of vitreoretinal traction on OCT, corresponding to the areas of leakage, were absent in the eyes analyzed in our series. Interestingly, we found the presence of areas of leakage in some patients that had undergone vitrectomy and peeling of EP and ILM for LMH several years previously (Fig. 11).
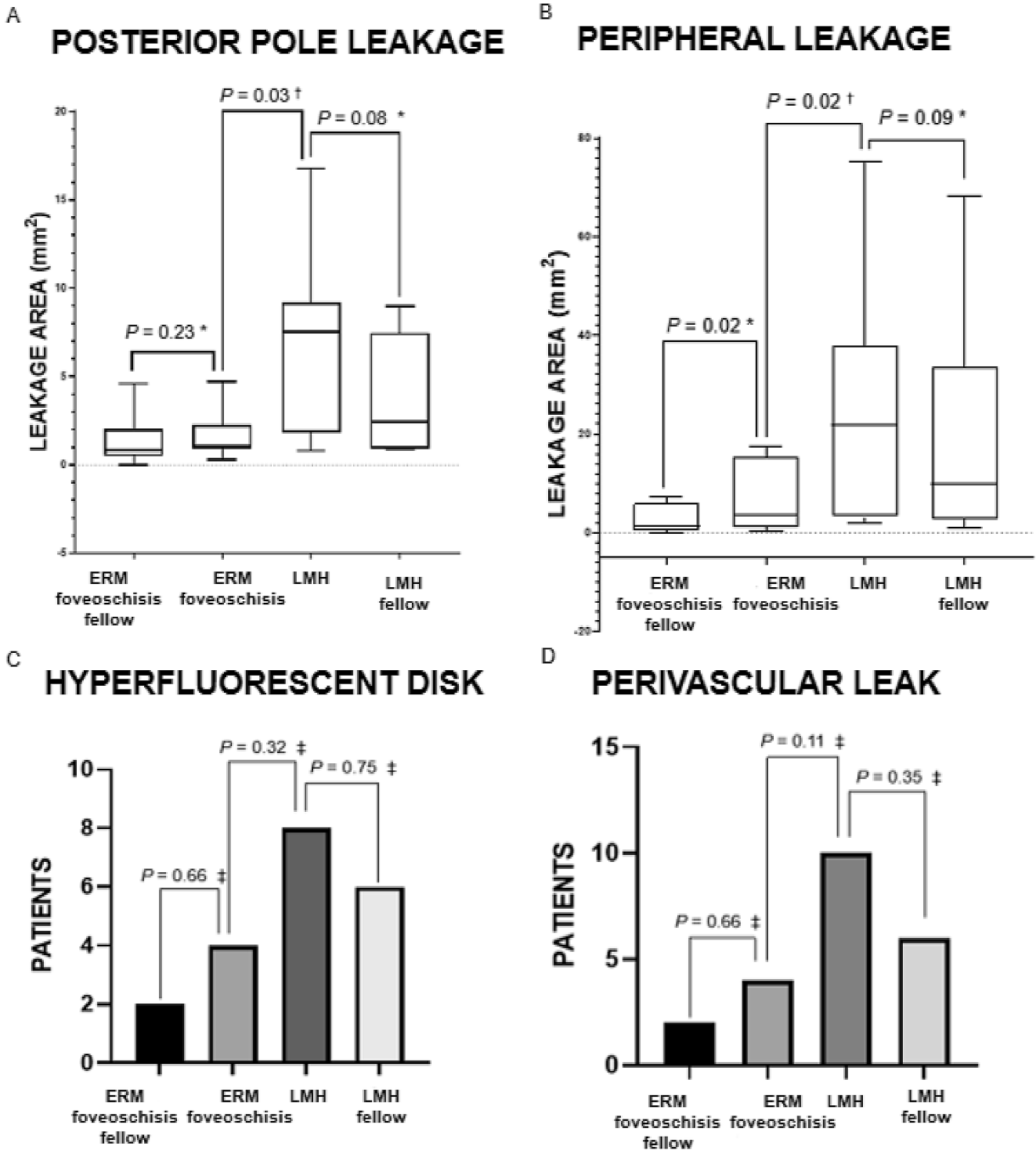
Figure 10. Comparison of fluorescein angiography findings in the study and fellow eyes of patients affected by lamellar macular holes and epiretinal membrane foveoschisis. (**A, B**) Box plots illustrating the areas of leakage at posterior pole and periphery. The horizontal lines within each box represent the median for each group, the ends of the boxes are the upper and lower quartiles, and the whiskers represent minimum and maximum values. (**C, D**) Bar graphs illustrating the number of patients with hyperfluorescent disk and perivascular leak for each group. * = Wilcoxon test; † = Mann-Whitney U test; ‡ = Fisher exact test.

In the absence of overt traction exerted by epiretinal membranes or vitreous on the retina, another possibility is that the bood retinal barrier breakdown evidenced by FA in our study was secondary to inflammation. In fact, we found signs of bilateral FA abnormalities (i.e. in both study and fellow eyes) in almost 70% of the patients examined. Some of these patients had leakage at both the posterior pole and periphery despite having only very mild sign of
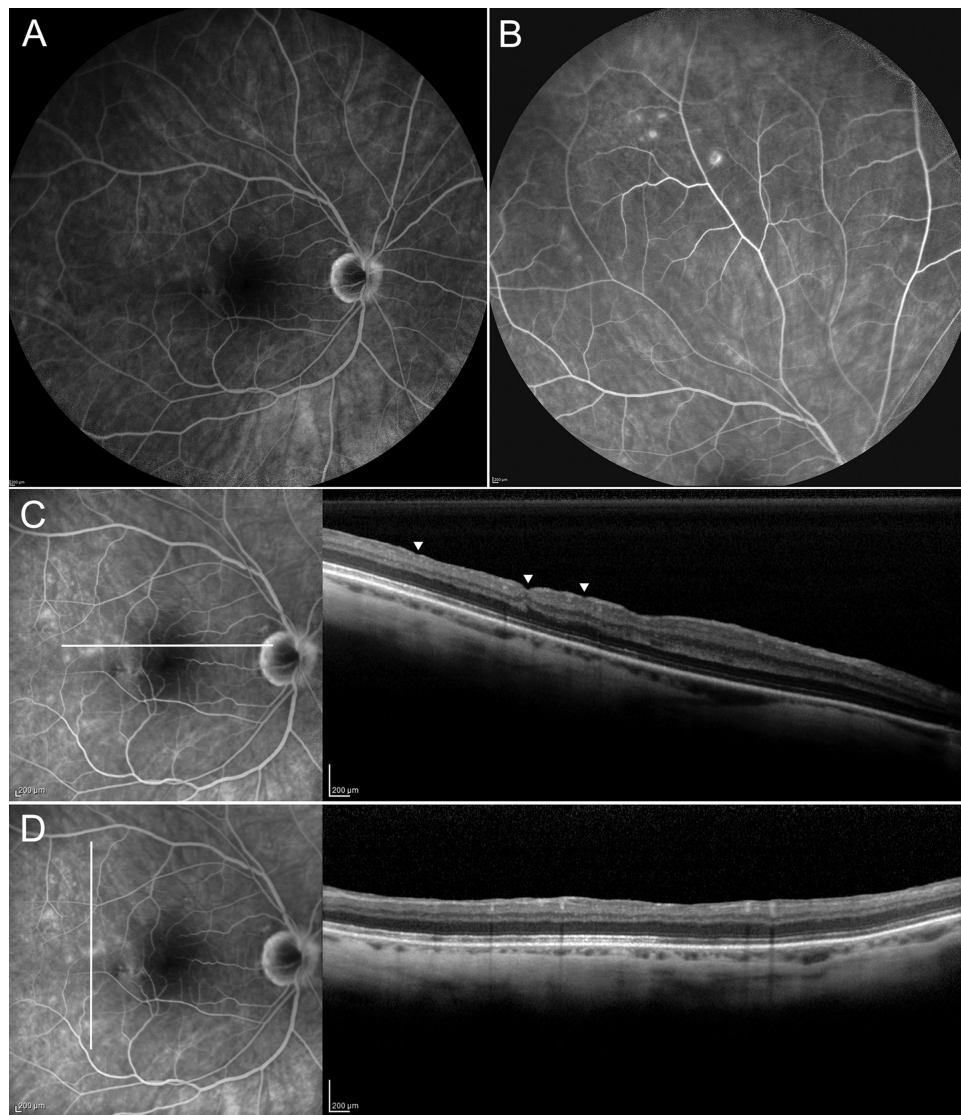
FIGURE 11. Fluorescein angiography (FA) and spectral-domain optical coherence tomography (SD-OCT) images recorded in a patient who had undergone pars plana vitrectomy and peeling of epiretinal proliferation/internal limiting membrane (ILM) for lamellar macular hole three years before. (**A, B**) On FA images, discrete areas of leakage are present at the posterior pole and at the periphery. The OCT images (with the related FA pics showing the level of the OCT scan) show the inner retinal dimplings, consequence of the ILM peeling (**C**) and the absence of signs of residual vitreoretinal traction corresponding to the areas of leakage on FA in either OCT scans (**C, D**).

macular epiretinal pathology (thin epiretinal membranes not associated with substantial distortion of the retinal profile), thus suggesting an underlying bilateral, subtle inflammatory state. Furthermore, all the eyes with LMH and more than half of those with ERM foveoschisis showed intraretinal HRDs, which have been previously interpreted as a sign of activation of microglial cells during inflammatory reactions.[38] Although it could be suggested that HRDs might be secondary to disruption of the ORB (observed in 58% of the LMH study eyes), with cosequent migration of RPE cells within the retina, it should be noted that all the LMH fellow eyes and 54.5% of the eyes with ERM foveoschisis (in which disruption of the ORB was respectively noted in 0 and 2 cases) presented with HRDs. On the other hand, we did not find any signs of inflammation in the vitreous either with slit lamp biomicroscopy or OCT. Further-

more, the general workup to exclude systemic inflammatory diseases causing secondary ocular involvement yielded negative results in all cases. Perhaps, it is possible that a low-grade inflammatory process, combined with age and concurrent vitreous changes, drives some of the mechanisms leading to the development of LMH and ERM foveoschisis. Aging and inflammation may act synergistically, precipitating disrupted homeostasis and activating the immunocompetent resident cells of the retina (astrocytes, Müller cells, microglia/macrophages, and RPE cells).[39] Müller cells dysfunction, in particular, may lead to a reduction in active potassium pumping, resulting in capillary dilation, and production of pro-permeabilizing cytokines, such as VEGF, IL-6, and MCP-1,[40] as well as other chemokines.[41] The resulting leakage might not always be widespread enough to cause retinal thickening or the formation of intraretinal cysts

visible on OCT. In these cases, the breakdown of the blood retinal barrier may be detectable only by FA, as shown in previous studies.[42–44]

Indeed, the presence of an underlying inflammatory state and the spontaneous fluctuations of its activity may explain some aspect of the natural history of LMH: first, the progressive thinning and loss of retinal tissue with disruption of the outer retinal layers; second, the possible evolution to full-thickness hole even in the absence of overt epiretinal traction forces; and third, the possible spontaneous improvement of the morphology and contour of the hole.[45]

Several limitations of this study are acknowledged. The sample size is small and an age-matched control group of patients with other vitreo-retinal interface disorders, or without retinal pathologies, is lacking. Therefore, it could be that, independently of the presence of LMH or ERM foveoschisis, FA abnormalities are more prevalent in older populations because of a vascular deterioration inevitably occurring with aging.

Thus, normative aging data are needed to confirm the mechanistic links proposed in this study. However, FA is an invasive examination with risk of potentially serious complications; thus, the use of healthy patients as controls may raise ethical concerns. Another limitation is that FA images were recorded without the use of ultrawide-field devices. Thus, it is possible that perfusion abnormalites in the far periphery were actually present, but failed to be detected in our sample. Another limitation is that the outlining of the areas of leakage was carried out manually and not using semi- or fully automatic tools. Finally, angio-OCT images were recorded in some patients but not systematically analyzed and compared with FA findings. Beyond the scope of the present work, we failed to find angio-OCT alterations either in the superficial or in the deep vascular plexuses that could explain the leakage observed on FA imaging. Further studies could clarify the relationship between abnormal FA findings and angio-OCT images in patients with LMH and ERM foveoschisis.

The strengths of this study include its prospective design and the potential information that FA may offer to better understand the pathogenesis of LMH and ERM foveoschisis. Although this research is preliminary in nature, we nevertheless believe it offers valuable insights, namely, that FA consistently revealed breakdown of the blood inner retinal barrier both at the posterior pole and periphery in eyes with LMH and ERM foveoschisis.

In conclusion, this study shows that several FA abnormalities may be found in eyes with LMH and ERM foveoschisis. Some of these abnormalities are a consequence of epiretinal tractional forces but others might be secondary to other underlying causes, including a subtle inflammatory process. Further studies involving larger samples are needed in order to validate our preliminary data and explore whether anti-inflammatory therapies, be they pharmacological or surgical, could change the natural course of these vitreomacular interface disorders.

Acknowledgments

References

1. Gass JD. Lamellar macular hole: a complication of cystoid macular edema after cataract extraction: a clinicopathologic case report. *Trans Am Ophthalmol Soc.* 1975;73:231–250.

2. Witkin AJ, Ko TH, Fujimoto JG, et al. Redefining lamellar holes and the vitreomacular interface: an ultrahigh-resolution optical coherence tomography study. *Ophthalmology.* 2006;113(3):388–397.

3. Parolini B, Schumann RG, Cereda MG, Haritoglou C, Pertile G. Lamellar macular hole: a clinicopathologic correlation of surgically excised epiretinal membranes. *Invest Ophthalmol Vis Sci.* 2011;52(12):9074–9083.

4. Duker JS, Kaiser PK, Binder S, et al. The International Vitreomacular Traction Study Group classification of vitreomacular adhesion, traction, and macular hole. *Ophthalmology.* 2013;120(12):2611–2619.

5. Pang CE, Spaide RF, Freund KB. Comparing functional and morphologic characteristics of lamellar macular holes with and without lamellar hole-associated epiretinal proliferation. *Retina.* 2015;35(4):720–726.

6. dell'Omo R, Virgili G, Rizzo S, et al. Role of lamellar hole-associated epiretinal proliferation in lamellar macular holes. *Am J Ophthalmol.* 2017;175:16–29.

7. Schumann RG, Compera D, Schaumberger MM, et al. Epiretinal membrane characteristics correlate with photoreceptor layer defects in lamellar macular holes and macular pseudoholes. *Retina.* 2015;35(4):727–735.

8. Compera D, Entchev E, Haritoglou C, et al. Lamellar hole-associated epiretinal proliferation in comparison to epiretinal membranes of macular pseudoholes. *Am J Ophthalmol.* 2015;160(2):373–384.e1.

9. Govetto A, Dacquay Y, Farajzadeh M, et al. Lamellar macular hole: two distinct clinical entities?. *Am J Ophthalmol.* 2016;164:99–109.

10. Gaudric A, Aloulou Y, Tadayoni R, Massin P. Macular pseudoholes with lamellar cleavage of their edge remain pseudoholes. *Am J Ophthalmol.* 2013;155(4):733–742.e7424.

11. Hubschman JP, Govetto A, Spaide RF, et al. Optical coherence tomography-based consensus definition for lamellar macular hole. *Br J Ophthalmol.* 2020;104(12):1741–1747.

12. Bottoni F, Carmassi L, Cigada M, Moschini S, Bergamini F. Diagnosis of macular pseudoholes and lamellar macular holes: is optical coherence tomography the "gold standard"? *Br J Ophthalmol.* 2008;92(5):635–639.

13. von Rückmann A, Fitzke FW, Gregor ZJ. Fundus autofluorescence in patients with macular holes imaged with a laser scanning ophthalmoscope. *Br J Ophthalmol.* 1998;82(4):346–351.

14. Klein BR, Hiner CJ, Glaser BM, Murphy RP, Sjaarda RN, Thompson JT. Fundus photographic and fluorescein angiographic characteristics of pseudoholes of the macula in eyes with epiretinal membranes. *Ophthalmology.* 1995;102(5):768–774.

15. Pang CE, Spaide RF, Freund KB. Epiretinal proliferation seen in association with lamellar macular holes: a distinct clinical entity. *Retina.* 2014;34(8):1513–1523.

16. Branson SV, McClafferty BR, Kurup SK. Vitrectomy for epiretinal membranes and macular holes in uveitis patients. *J Ocul Pharmacol Ther.* 2017;33(4):298–303.

17. Jabs DA, Nussenblatt RB, Rosenbaum JT; Standardization of Uveitis Nomenclature (SUN) Working Group. Standardization of uveitis nomenclature for reporting clinical data. Results of the First International Workshop. *Am J Ophthalmol.* 2005;140(3):509–516.

18. Nussenblatt RB, Palestine AG, Chan CC, Roberge F. Standardization of vitreal inflammatory activity in intermediate and posterior uveitis. *Ophthalmology.* 1985;92(4):467–471.

19. Schneider CA, Rasband WS, Eliceiri KW. NIH Image to ImageJ: 25 years of image analysis. *Nat Methods.* 2012;9(7):671–5.

20. Keane PA, Karampelas M, Sim DA, et al. Objective measurement of vitreous inflammation using optical coherence tomography. *Ophthalmology.* 2014;121(9):1706–1714.

21. Haouchine B, Massin P, Tadayoni R, Erginay A, Gaudric A. Diagnosis of macular pseudoholes and lamellar macular holes by optical coherence tomography. *Am J Ophthalmol.* 2004;138(5):732–739.

22. Bottoni F, Deiro AP, Giani A, Orini C, Cigada M, Staurenghi G. The natural history of lamellar macular holes: a spectral domain optical coherence tomography study. *Graefes Arch Clin Exp Ophthalmol.* 2013;251(2):467–475.

23. Figueroa MS, Noval S, Contreras I. Macular structure on optical coherence tomography after lamellar macular hole surgery and its correlation with visual outcome. *Can J Ophthalmol.* 2011;46(6):491–497.

24. Michalewska Z, Michalewski J, Sikorski BL, et al. A study of macular hole formation by serial spectral optical coherence tomography. *Clin Exp Ophthalmol.* 2009;37(4):373–383.

25. Nguyen JH, Yee KMP, Nguyen-Cuu J, Sebag J. Structural and functional characteristics of lamellar macular holes. *Retina.* 2019;39(11):2084–2089.

26. Maguire AM, Margherio RR, Dmuchowski C. Preoperative fluorescein angiographic features of surgically removed idiopathic epiretinal membranes. *Retina.* 1994;14(5):411–416.

27. Liu J, Qian Y, Yang S, et al. Pathophysiological correlations between fundus fluorescein angiography and optical coherence tomography results in patients with idiopathic epiretinal membranes. *Exp Ther Med.* 2017;14(6):5785–5792.

28. Johnson MW. Tractional cystoid macular edema: a subtle variant of the vitreomacular traction syndrome. *Am J Ophthalmol.* 2005;140(2):184–192.

29. Irvine SR. A newly defined vitreous syndrome following cataract surgery. *Am J Ophthalmol.* 1953;36(5):599–619.

30. Severin SL. Late cystoid macular edema in pseudophakia. *Am J Ophthalmol.* 1980;90(2):223–225.

31. Hernández-Rodríguez J, Hoffman GS. Updating single-organ vasculitis. *Curr Opin Rheumatol.* 2012;24(1):38–45.

32. Jennette JC, Falk RJ, Bacon PA, et al. 2012 revised International Chapel Hill Consensus Conference Nomenclature of Vasculitides. *Arthritis Rheum.* 2013;65:1–11.

33. Graham EM, Stanford MR, Sanders MD, Kasp E, Dumonde DC. A point prevalence study of 150 patients with idiopathic retinal vasculitis: 1. Diagnostic value of ophthalmological features. *Br J Ophthalmol.* 1989;73(9):714–721.

34. George RK, Walton RC, Whitcup SM, Nussenblatt RB. Primary retinal vasculitis. Systemic associations and diagnostic evaluation. *Ophthalmology.* 1996;103(3):384–389.

35. Maleki A, Cao JH, Silpa-Archa S, Foster CS. Visual outcome and poor prognostic factors in isolated idiopathic retinal vasculitis. *Retina.* 2016;36(10):1979–1985.

36. Sullu Y, Sariaydin G, Kuruoglu S, Beden U. Widespread vitreoretinal traction simulating retinal vasculitis in a patient with uveitis. *Retin Cases Brief Rep.* 2012;6(4):379–382.

37. Tranos PG, Errera MH, Vakalis AN, Asteriades SG, Pavesio C. Pseudovasculitis associated with vitreoretinal traction. *Retin Cases Brief Rep.* 2012;6(2):219–221.

38. Coscas G, De Benedetto U, Coscas F, et al. Hyperreflective dots: a new spectral-domain optical coherence tomography entity for follow-up and prognosis in exudative age-related macular degeneration. *Ophthalmologica.* 2013;229(1):32–37.

39. Daruich A, Matet A, Moulin A, et al. Mechanisms of macular edema: beyond the surface. *Prog Retin Eye Res.* 2018;63:20–68.

40. Eastlake K, Banerjee PJ, Angbohang A, Charteris DG, Khaw PT, Limb GA. Müller glia as an important source of cytokines and inflammatory factors present in the gliotic retina during proliferative vitreoretinopathy. *Glia.* 2016;64(4):495–506.

41. Rutar M, Natoli R, Chia RX, Valter K, Provis JM. Chemokine-mediated inflammation in the degenerating retina is coordinated by Müller cells, activated microglia, and retinal pigment epithelium. *J Neuroinflammation.* 2015;12:8.

42. Tran TH, de Smet MD, Bodaghi B, Fardeau C, Cassoux N, Lehoang P. Uveitic macular oedema: correlation between optical coherence tomography patterns with visual acuity and fluorescein angiography. *Br J Ophthalmol.* 2008;92(7):922–927.

43. Brar M, Yuson R, Kozak I, et al. Correlation between morphologic features on spectral-domain optical coherence tomography and angiographic leakage patterns in macular edema. *Retina.* 2010;30(3):383–389.

44. Kozak I, Morrison VL, Clark TM, et al. Discrepancy between fluorescein angiography and optical coherence tomography in detection of macular disease. *Retina.* 2008;28(4):538–544.

45. Lai TT, Chen SN, Yang CM. Epiretinal proliferation in lamellar macular holes and full-thickness macular holes: clinical and surgical findings [published correction appears in Graefes Arch Clin Exp Ophthalmol. 2016 Apr;254(4):823]. *Graefes Arch Clin Exp Ophthalmol.* 2016;254(4):629–638.